Preparation and characterisation of controlled porosity alginate hydrogels made via a simultaneous micelle templating and internal gelation process

S. Partap · A. Muthutantri · I. U. Rehman ·
G. R. Davis · J. A. Darr

Abstract Controlled porosity alginate hydrogel monoliths were synthesised by simultaneous micelle templating (MT) and an internal gelation reaction. In water, the self assembling surfactant, cetyltrimethy-lammonium bromide (CTAB) formed non-spherical micelles that were used as a template for pore formation. The porous microstructure was assessed by mercury intrusion porosimetry (MIP), helium pycnometry, X-ray microtomography (XMT) and scanning electron microscopy (SEM), respectively. The MT hydrogels displayed relatively monodisperse pore size distributions (with pore sizes ranging from 32.5 μm to 164.0 μm), high total pore volumes (4.5–20.3 cm^3/g) and high degrees of porosity (83–97%). Some control over pore size distributions was achieved by varying the surfactant concentration; higher surfactant concentrations, led to smaller pores with lower total pore volumes. Uniaxial compression testing revealed that hydrogels made via MT are stable in cell culture media for 28 days. Fourier transform infrared (FTIR) spectroscopy data, suggested that all surfactant could be removed from the final product by washing with ethanol and water, making these hydrogels potentially suitable for tissue engineering (TE) applications.

Introduction

Tissue engineering (TE) requires the formation of highly porous materials with open and interconnected pore networks, ideally with controllable pore size distributions to allow for cell migration, nutrient delivery and waste elimination [1–3]. Hydrogels are especially appealing for TE applications as they are analogous to the natural extracellular matrix of soft tissues. They are three dimensional polymeric networks capable of absorbing large quantities of water [4], and are widely used in the biomedical field as drug delivery devices, wound dressings, contact lenses and scaffolds for TE [1, 4–6].

Alginate is a particularly attractive natural biomaterial [7, 8]; being well-known for its good biocompatibility, low toxicity and mild gelation chemistry with Group 2 metal cations (usually Ca^{2+} ions). Freeze-drying [9, 10], particulate leaching [11], gas foaming methods (e.g. using supercritical fluids) [12, 13] and the use of gas forming agents [14, 15] (amongst others) are used to synthesise porous polymers or hydrogels. However, these methods often yield hydrogels with broad macropore size distributions with a mixture of open and closed pores [16], whilst, emulsion templating methods can give polymers with well defined and controlled pore structures [17–21]. Surfactant or micelle templating is another type of templating reaction which

S. Partap · A. Muthutantri · J. A. Darr (✉)
Department of Materials, Queen Mary University
of London, Mile End, London E1 4NS, UK
e-mail: j.a.darr@qmul.ac.uk

I. U. Rehman
IRC in Biomedical Materials, Queen Mary University
of London, Mile End, London E1 4NS, UK

G. R. Davis
Dental Biophysics Section, Institute of Dentistry,
Queen Mary University of London, Mile End Road,
London E1 4NS, UK

is based on the self assembly of surfactants to form micelles. Cetyltrimethylammonium bromide (CTAB) is one such surfactant that is known to self assemble into micelles in water [22, 23], and has been widely used to synthesise mesoporous materials with narrow pore size distributions for use as catalysts and molecular sieves [24, 25].

In this work, self assembled CTAB micelles in water were used as templates around which gelation of alginate (crosslinking) occurred, for the generation of controlled porosity hydrogels. The surfactant could subsequently be removed to give hydrogels which are potentially suitable for tissue engineering applications. A general reaction scheme for the synthesis of porous alginate hydrogel monoliths is shown in Fig. 1. In all reactions, complexed calcium ions were dispersed in a sodium alginate solution, to which an aqueous CTAB mixture was added. Subsequently, an acid was added to release the calcium ions and crosslink the sodium alginate using the carboxylate anions on the alginate backbone (albeit in the presence of the templating micelles) to yield a porous alginate hydrogel.

Materials

All chemicals were purchased from Aldrich Chemical Company (Dorset, UK) unless otherwise specified. Adipic acid (high purity, 99 %), sodium citrate dihydrate (99+ %), cetyltrimethylammonium bromide (CTAB) (99 %), Protanal LF 10/60 sodium alginate, (M_w of 120,000–180,000, G content 65–75%, pharmaceutical grade, Honeywill & Stein Ltd. UK), calcium carbonate (min 99% AnalaR grade, BDH, UK), ethanol (99.7% BDH, UK).

Methods

About 0.50 g calcium carbonate and 0.98 g trisodium citrate were added to 50 mL distilled water (to form a 0.1 M calcium solution) by stirring on a heated magnetic stirrer for 15 min at 50 °C. 4.0 g sodium alginate was added very slowly to the stirred solution to give an 8% w/v solution (mixed with an overhead stirrer). Once a homogeneous dispersion of alginate was obtained, 30 mL of an aqueous solution (0.29, 1.10, 5.47 or 8.75 g CTAB dissolved in 30 mL distilled water) was added very slowly to the alginate solution under stirring to give a final CTAB concentration of 0.01 M, 0.04 M, 0.2 M or 0.3 M, respectively. For hydrogels made at 35 °C (samples 2, 4, 6, and 8 in Table 1), the sodium alginate solution was first prepared at 50 °C and then cooled, prior to the addition of the aqueous CTAB solution. Finally, adipic acid solution (0.73 g adipic acid dissolved in 10 mL distilled water at 70 °C) was added whilst being stirred. The solution was left to stir until it became viscous, after which time it was left to stand for 24 h.

Hydrogels made with potassium bromide (KBr) were made at 50 °C; 0.95, 0.48 or 0.10 g of KBr (samples 9, 10 and 11, respectively; see Table 1) was added to a 0.01 M aqueous CTAB solution to make up 0.01, 0.05 and 0.1 M KBr concentrations, respectively. This mixed solution was then added to the sodium alginate solution and the reaction proceeded from there on as stated for the earlier reactions. Finally, the hydrogels were soaked in 100% ethanol for 1 h at 40 °C and then soaked in distilled water for an additional 24 h, where the water was exchanged twice, approximately every 12 h. The hydrogel was then frozen at –50 °C and freeze dried for 18 h at 12×10^{-3} Torr.

Characterisation

For scanning electron microscopy (SEM) analyses, freeze dried samples were immersed in liquid nitrogen for five minutes, fractured into smaller pieces with a sharp razor blade and then mounted on aluminium stubs with carbon black paste. Samples were coated with gold (Agar Auto Sputter Coater 103A) before analysis using the JEOL 6300F SEM with an accelerating voltage of 10 KeV.

Prior to X-ray microtomography (XMT) 5 mm³ foam samples were placed in plastic vials with a desicant. The samples were glued onto a piece of cardboard that was used to separate the sample from the

Fig. 1 Reaction scheme for the synthesis of porous alginate hydrogels made using simultaneous micelle templating (MT) and internal gelation
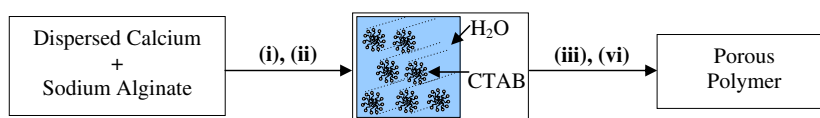
Key: (i) premix alginate solution with complexed calcium; (ii) add an aqueous cetyltrimethylammonium bromide (CTAB) solution, and in selected cases add KBr; (iii) add an acid and leave for 24 hrs; (vi) wash and freeze-dry.

Table 1 Mercury intrusion porosimetry (MIP) and helium pycnometry data for porous alginate hydrogels made using simultaneous micelle templating and internal gelation at 50 °C

	Concentration of CTAB/M	Concentration of KBr/M	Modal pore diameter (μm)	Total pore volume (cm^3/g)	Total porosity [26]
1	0.3	0	45.4	5.1	90
2[a]	0.3	0	32.5	4.5	83
3	0.2	0	40.6	5.7	83
4[a]	0.2	0	52.8	8.1	86
5	0.04	0	77.0	9.9	89
6[a]	0.04	0	80.7	12.2	91
7	0.01	0	119.4	16.2	95
8[a]	0.01	0	102.9	20.3	89
9	0.01	0.01	164.0	5.8	97
10	0.01	0.05	120.1	10.4	95
11	0.01	0.1	126.6	13.0	94

[a] Samples made at 35 °C

dessicant (and to keep them from moving whilst being imaged). The samples were imaged with a XMT unit constructed by Davis [27] using a X-Tek (UK) 160 kV Ultrafocus X-ray source system. A voxel size of 14.89 μm was used with an exposure time of 10 s. Precisely 701 projections were collected and the re-constructed volumes consisted of $460 \times 490 \times 212$ voxels. The samples were rotated 360° with the image acquisition times ranging from 9.5 h to 10 h for each sample. Data collection and volume reconstruction was performed on software written by Davis. VGStudio-Max was used to render the images to produce three dimensional images.

Mercury intrusion porosimetry (MIP) was per-formed using the Autopore 9510 porosimeter (Micromeritics). Low-pressure intrusion porosimetry (0–45 psi) was employed to obtain interconnected macropore diameter distributions in the range of 1–360 μm. The skeletal density was determined by automated helium displacement pycnometry using the Accupyc 1330 (Micromeritics) using a known mass of foam.

To monitor the degradation properties, gel disks (12 mm diameter and 6 mm thicknesses) were incu-bated in Dulbeccos's modified eagles medium (DMEM) at 37 °C for 4 weeks. At specified time points (days 0, 1, 4, 7, 14 and 28) six specimens of each sample type were removed for testing; uniaxial com-pression tests were performed on an Instron 5564 mechanical tester (Instron Corporation) with a 100 N load cell. The compressive strain was set to a maximum of 50% and testing was carried out at a speed of 3.6 mm/min (initial strain rate of 0.01 s^{-1}). Extension (mm) and load (N) were recorded using Merlin^{TM} materials testing software (Instron Corporation). The compressive elastic moduli of the gels were calculated from the stress-strain curves limited to the first 10% of strain [28–30]. The cell culture media was exchanged once a week throughout the study.

Fourier transform infra red (FTIR) spectra were recorded on a Nicolet 800 spectrometer in conjunction with a diffuse reflectance infrared Fourier transform sampling (DRIFTS) cell. Spectra were collected be-tween 400 cm^{-1} and 4,000 cm^{-1} with 32 scans and a spectral resolution of 4 cm^{-1}. Samples were ground into a fine powder and diluted with approximately 20% potassium bromide.

Results and discussion

SEM, MIP, helium pycnometry and XMT were used to assess the microstructure of the templated foams. Results showed that the micelle templating (MT) technique coupled to internal gelation, produced por-ous hydrogels with open and interconnected pore networks. SEM and XMT show that pores in the MT samples are fairly uniform in both shape and size and are arranged in an ordered manner. The SEM images also show that the MT samples display signs of a "tubular" or elongated pore structure, especially seen in Fig. 2a. In addition, the images suggest that as the surfactant concentration increases, the pores appear to get smaller and more closed. MIP and helium pyc-nometry showed that hydrogels made via MT produced highly porous (83–97%) hydrogels with high total pore volumes (4.5–20.3 cm^3/g), and very uniform and monodisperse pore size distributions (Figs. 3, 4), with pore sizes for all samples in the range of 32.5–164.0 μm. The degree of control over the pore size distributions seen by using the MT technique was not always evident in our previously reported work [21], where an "oil-in-water" (o/w) emulsion template was used to synthesise porous alginate hydrogels. Such
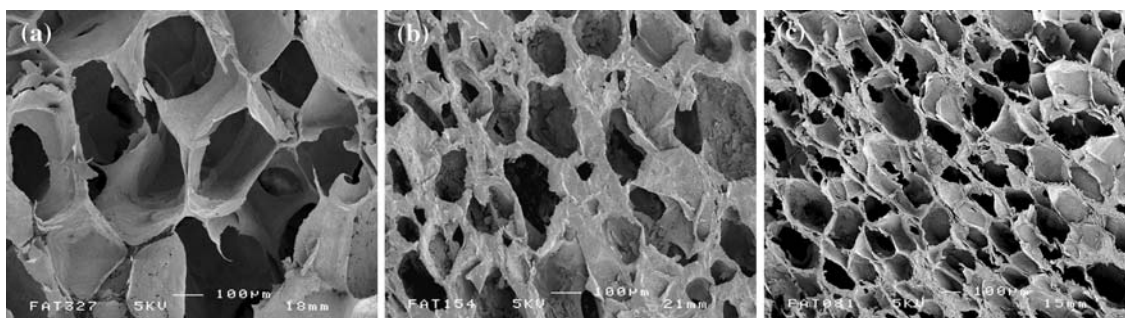
Fig. 2 Scanning electron microscopy (SEM) images of hydrogels made via simultaneous micelle templating and internal gelation at 50 °C, using CTAB concentrations of (**a**) 0.04 M, (**b**) 0.2 M and (**c**) 0.3 M (samples 5, 3 and 1, respectively)
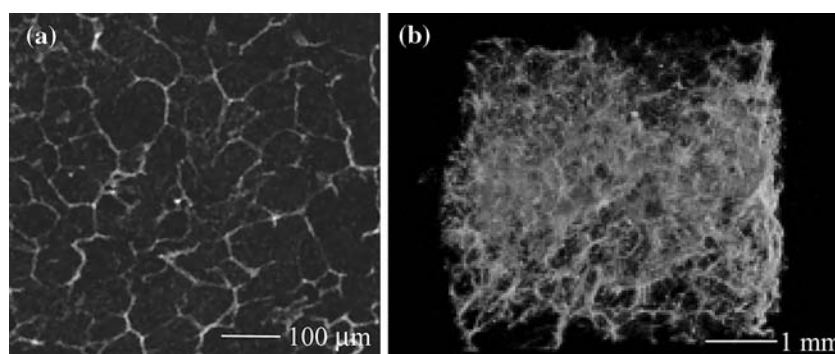

Fig. 3 (**a**) Two dimensional and (**b**) three dimensional X-ray microtomography (XMT) images of hydrogels made at 50 °C via simultaneous micelle templating and internal gelation, using a 0.01 M CTAB concentration

hydrogels were 79–97% porous (range) with total pore volumes in the range of 1.7–5.9 cm^3/g, with fairly broad pore size distributions. Furthermore, when we previously reported the replacement of the organic solvent in the o/w emulsion with carbon dioxide, some control over the pore size distributions was observed by varying the surfactant concentration. Those hydrogels were 78–95% porous, with total pore volumes in the range 2.7–9.4 cm^3/g [21].

Pore size distributions were also controlled in the MT hydrogels by varying the surfactant concentration. At low concentrations (0.01 M CTAB), open, interconnected and slightly elongated pores with higher total pore volumes and larger pore sizes were observed (Fig. 4d, e). At higher surfactant concentrations (e.g. 0.3 M CTAB), the pore network appeared to become more closed with smaller pores; in addition, narrower pore size distributions with reduced pore volumes were observed (Fig. 4a). It has been observed elsewhere that at high surfactant concentrations it can become more favourable for micelles to grow axially into tubular micelles [31]. Experiments were also performed here where it was expected that the addition of a salt (potassium bromide) would encourage the "sphere to rod" transition at low surfactant concentrations (0.01 M). The addition of potassium bromide reduced

the total pore volumes of the samples, but did not appear to affect the pore size distributions significantly (Fig. 4e and Table 1). The added salt may have altered the surface charge density of the micelles to reduce the head group repulsions, which decreased the separation between micelles, encouraging the elongation of the spherical micelles [32–34]. However, under the conditions employed herein, it was not conclusive as to whether the "sphere to rod" transition actually occurred.

Two different temperatures (35 and 50 °C) were investigated to see the influence upon the resulting pore morphology; at higher temperatures, wormlike micelles are known to "melt" and not form properly [35]. Therefore, a lower temperature of 35 °C was used for selected reactions, as the micelles would be expected to be more stable under these conditions. No significant effect of temperature was observed with regards to the pore size distributions (Table 1 and Fig. 4).

The stability of the hydrogels was monitored in cell culture media over four weeks. All samples were stable throughout the four week time period without any significant degradation (Fig. 5). Gels made with lower concentrations of surfactant (0.04 and 0.2 M) showed a general increase in compressive modulus with

Fig. 4 Mercury intrusion porosimetry (MIP) data for hydrogels made via simultaneous micelle templating and internal gelation, using CTAB concentrations of (**a**) 0.3 M (sample 1 and 2), (**b**) 0.2 M (sample 3 and 4), (**c**) 0.04 M (sample 5 and 6) and (**d**) 0.01 M (sample 7 and 8). (**a**)–(**d**) Show plots of hydrogels made at 35 and 50 °C, respectively. (**e**) Shows MIP plots for porous hydrogels made at 50 °C, using 0.01 M CTAB with 0.01 (sample 9), 0.1 (sample 10) and 0.5 M (sample 11) potassium bromide solutions, respectively. For comparison, (**e**) also shows the MIP plot for sample 8
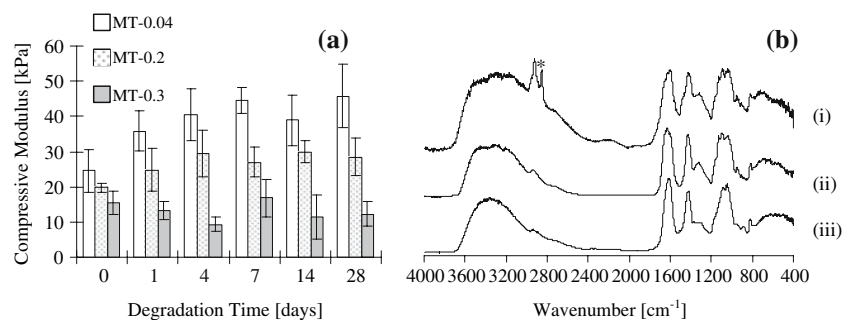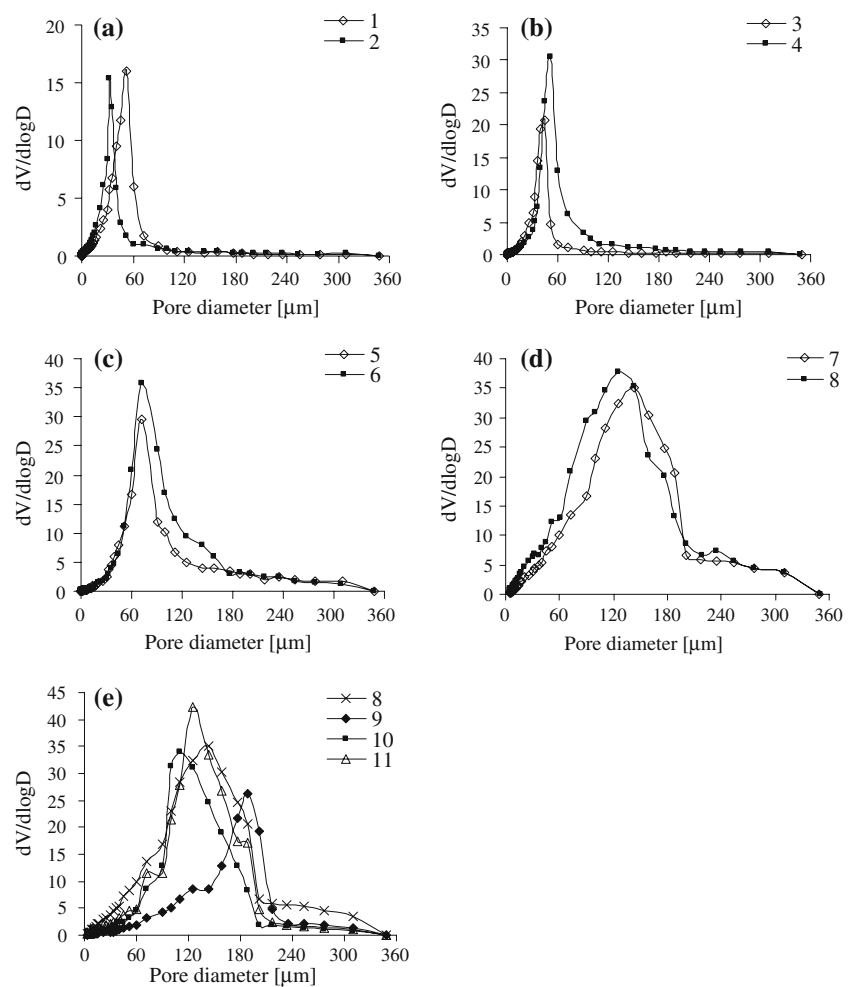

Fig. 5 (**a**) Compressive modulus as a function of degradation time for porous hydrogels (made using 0.04, 0.2 and 0.3 M CTAB concentrations for samples 5, 3 and 1, respectively) incubated in Dulbeccos's modified eagles medium (DMEM) at 37 °C and, (**b**) Fourier transform infrared (FTIR) spectra of a porous alginate hydrogels made at 50 °C; (i) unwashed sample after micelle templating (0.3 M CTAB) and internal gelation, (ii) washed sample after micelle templating (0.3 M CTAB) and internal gelation, and (iii) a control sample, where internal gelation was carried out in the absence of surfactant

degradation time. This could possibly be due to the free calcium ions (in cell culture media) that were able to increase the extent of crosslinking. However, gels made at high concentrations of surfactant (0.3 M) were more fragile to handle and were whiter in appearance than those at 0.01 M CTAB; this indicates that a high concentration of surfactant possibly interfered with the gelling mechanism. In addition, the 0.3 M CTAB samples deformed plastically when subjected to a small compressive load, whereas, those made at low concentrations of surfactant, recovered somewhat after the load was removed.

FTIR spectroscopy was used to confirm that residual surfactant could be washed out. The hydrogels were soaked in 100% ethanol for 1 h at 40 °C, and then soaked in distilled water for 24 h, where the water was exchanged twice a day (every 12 h). In all spectra, the peaks were assigned as follows; the broad peak at 3,303 cm^{-1} is characteristic of O–H stretching, the peak at 2,900 cm^{-1} is characteristic of C–H stretching, the asymmetric and symmetric stretches of the COO$^-$ group of alginate are located at 1,620 cm^{-1} and 1,433 cm^{-1}, respectively [36–38]. The peaks at 1,146, 1,086 and 1,045 cm^{-1}, respectively correspond to C–C stretching, C–O stretching and O–H bending [37, 39, 40]. In Fig. 5b(i), a doublet at 2,923 and 2,854 cm^{-1} (designated by an asterisk) is assigned to the C–H stretching bands of CH$_3$ and CH$_2$, respectively of the CTAB surfactant [41–43]. These peaks disappear after the hydrogels were washed with ethanol/water, showing that all residual surfactant could be washed out [Fig. 5b(ii)].

In conclusion, highly porous alginate hydrogels were made using a simultaneous micelle templating and internal gelation technique. The porous alginate hydrogels had monodisperse pore sizes with high total pore volumes. The pore structure could be controlled by varying the surfactant concentration; low surfactant concentrations lead to larger pores and higher total pore volumes. Future work will concentrate on the biological assessment of these hydrogels, in terms of assessing their biocompatibility and suitability for tissue engineering applications. This will be reported in due course.

References

1. Drury JL, Mooney DJ (2003) Biomaterials 24:4337
2. Hutmacher DW (2000) Biomaterials 21:2529
3. Hollister SJ, Maddox RD, Taboas JM (2002) Biomaterials 23:4095
4. Hoffman AS (2002) Adv Drug Deliv Rev 54:3
5. Peters MC, Isenberg BC, Rowley JA, Mooney DJ (1998) J Biomater Sci Polym Ed 9:1267
6. Langer R, Peppas NA (2003) Aiche J 49:2990
7. Ju HK, Kim SY, Lee YM (2001) Polymer 42:6851
8. Lee KY, Mooney DJ (2001) Chem Rev 101:1869
9. Whang K, Thomas CH, Healy KE, Nuber G (1995) Polymer 36:837
10. Zmora S, Glicklis R, Cohen S (2002) Biomaterials 23:4087
11. Chen GP, Ushida T, Tateishi T (2001) Biomaterials 22:2563
12. Sheridan MH, Shea LD, Peters MC, Mooney DJ (2000) J Control Release 64:91
13. Mooney DJ, Baldwin DF, Suh NP, Vacanti LP, Langer R (1996) Biomaterials 17:1417
14. Eiselt P, Yeh J, Latvala RK, Shea LD, Mooney DJ (2000) Biomaterials 21:1921
15. Choi BY, Park HJ, Hwang SJ, Park JB (2002) Int J Pharm 239:81
16. Kawanishi M, Ushida T, Kaneko T, Niwa H, Fukubayashi T, Nakamura K, Oda H, Tanaka S, Tateishi T (2004) Mater Sci Eng C 24:431
17. Cameron NR (2005) Polymer 46:1439
18. Busby W, Cameron NR, Jahoda CAB (2001) Biomacro-molecules 2:154
19. Butler R, Davies CM, Cooper AI (2001) Adv Mater 13:1459
20. Butler R, Hopkinson I, Cooper AI (2003) J Am Chem Soc 125:14473
21. Partap S, Darr JA, Jones JR, Rehman I (2006) Adv Mater 18:501
22. Song WL, Li A, Xu XQ (2003) Ind Eng Chem Res 42:949
23. Kim WJ, Yang SM (2000) J Colloid Interface Sci 232:225
24. Ruckenstein E, Chao ZS (2001) Nano Lett 1:739
25. Xu J, Luan ZH, He HY, Zhou WZ, Kevan L (1998) Chem Mater 10:3690
26. Davis GR, Elliott JC (2003) J Phys IV France 104:131
27. Kong HJ, Lee KY, Mooney DJ (2002) Polymer 43:6239
28. Moresi M, Mancini M, Bruno M, Rancini R (2001) J Text Stud 32:375
29. Mitchell JR (1980) J Text Stud 11:315
30. Da Rocha PSR, Harrison KL, Johnston KP (1999) Langmuir 15:419
31. Schubert BA, Kaler EW, Wagner NJ (2003) Langmuir 19:4079
32. Vinson PK, Bellare JR, Davis HT, Miller WG, Scriven LE (1991) J Colloid Interface Sci 142:74
33. Subramanian V, Ducker WA (2000) Langmuir 16:4447
34. Kim WJ, Yang SM, Kim M (1997) J Colloid Interface Sci 194:108
35. Cates ME, Candau SJ (1990) J Phys Condens Matter 2:6869
36. Fourest E, Volesky B (1996) Environ Sci Technol 30:277
37. Sartori C, Finch DS, Ralph B, Gilding K (1997) Polymer 38:43
38. Kadokawa J, Saitou S, Shoda S (2005) Carbohydr Polym 60:253
39. Wasikiewicz JM, Yoshii F, Nagasawa N, Wach RA, Mitomo H (2005) Radiat Phys Chem 73:287
40. Pereira L, Sousa A, Coelho H, Amado AM, Ribeiro-Claro PJA (2003) Biomol Eng 20:223
41. Li HY, Tripp CP (2004) Langmuir 20:10526
42. Li HY, Tripp CP (2004) J Phys Chem B 108:18318
43. Ford C, Singh M, Lawson L, He JB, John V, Lu YF, Papadopoulos K, Mcpherson G, Bose A (2004) Colloids Surf B 39:143